The 8th European Congress on Computational Methods in Applied Sciences and Engineering
ECCOMAS Congress 2022
5-–9 June 2022, Oslo, Norway

FULLY-DISCRETE ENTROPY CONSERVING/STABLE DISCONTINUOUS GALERKIN SOLVER FOR UNSTEADY COMPRESSIBLE VISCOUS FLOWS

A. COLOMBO[1], A. CRIVELLINI [2] AND A. NIGRO[2]

[1] University of Bergamo
Department of Engineering and Applied Sciences
e-mail: alessandro.colombo@unibg.it

[2] Marche Polytechnic University
Department of Industrial Engineering and Mathematical Sciences
email: a.crivellini@univpm.it, a.nigro@univpm.it

Key words: Discontinuous Galerkin, entropy variables, entropy conserving/stable numerical fluxes, generalized Crank-Nicolson time integration.

Abstract. The aim of this work is to contribute to the development of a high-order accurate discretization that is entropy conserving and entropy stable both in space and in time. To do this, the general framework is based on a high-order accurate discontinuous Galerkin (dG) method in space with entropy working variables, several entropy conservative and stable numerical fluxes and an entropy conserving modified Crank-Nicolson method. We present the first results, obtained with the discretizations here proposed, for two bi-dimensional unsteady viscous test-case: the Taylor-Green vortex and the double shear layer.

1 INTRODUCTION

In the last years entropy-conserving (EC) and entropy-stable (ES) methods have attracted much interest. The idea to ensure at a discrete level the conservation/stability of entropy dates back to 80s with the first works of Tadmor, Harten and Hughes et al. [1, 2, 3, 4, 5].

Since these early works, high-order methods, and among them the discontinuous Galerkin (dG) methods, have attracted significant attention, even if the debate about the superior performance of high-order methods with respect to low-order ones is still on today. The main reasons that have promoted the development of high-order methods are the higher accuracy that they possess per degree of freedom (DoF) and the smaller numerical dispersion and dissipation errors with respect to low-order methods [6, 7], properties that make these methods an optimal candidate to solve simulations of turbulent flows. On the other hand, the main drawbacks of high-order methods are the higher CPU time required per DoF with respect to low-order methods, and their loss of robustness for discontinuous solutions or when some physical features are strongly under-resolved, which is really common for turbulent flows (ILES/uDNS). Note that, at this regards, entropy stable schemes improve the robustness of numerical schemes, in fact, as demonstrated in [8] and reported in [9], dG methods are stable for linear problem, but, for scalar nonlinear hyperbolic problems, they are L_2-stable only if the following conditions hold:

i) all integrals must be evaluated exactly; ii) an entropy stable numerical flux is used at element interfaces.

Starting from the seminal works of 80s [1, 2, 3, 4, 5], several entropy conservative and entropy stable Riemann solvers [10, 11, 12] and several dG formulations in entropy variables [13, 14, 15] have been developed. In particular, note that in the last works it is adopted a space-time dG formulation in which all the space and time DoFs are coupled, which clearly leads to a more CPU time consuming method with respect to the one required with the method of lines, which is the method here proposed. A framework to construct high-order EC schemes in periodic domains has been given by LeFloch et al. [16]. Fisher and Carpenter [17] combined this approach with SBP operators proving that, when the derivative approximations in space are SBP operators, two-point EC fluxes can be used to construct high-order schemes. Gassner et al. [18, 19] showed that, when specific numerical volume fluxes in the flux form volume integral of Fisher and Carpenter are chosen, skew-symmetric-like (split form) DGSEM formulations for the Euler equations can be discretely recovered. It should be mentioned that most of the described EC and ES approaches have been developed for semi-discrete Navier-Stokes equations and, to the best of authors knowledge, it seems that until now the attention has been focused mainly on the spatial discretization, since only few works have been developed for fully-discrete system of equations with these properties [16, 20, 21, 22, 23]. Nevertheless, even if EC or ES formulations in space are used, it is not possible to ensure that these properties are fulfilled for time-dependent solutions, for which there is a not negligible effect due to the accuracy of the time integration method used.

In this work we want to contribute to the development of high-order accurate fully-discrete entropy conserving/stable schemes, extending the work presented in [24, 25] to viscous flows. The aim is to couple the desirable properties of high-order methods with the superior robustness given by entropy stable schemes, and the final target is to perform high-fidelity simulations of complex turbulent flow phenomena with a reduced CPU time. The general framework is a modal high-order dG discretization in space with entropy working variables, several entropy conservative and stable numerical fluxes and an implicit time integration method that is entropy conservative. In particular, the discretization in time is performed with a generalized Cranck-Nicolson method, which has been inspired by [16, 20, 21] and adapted to the dG discretization with entropy variables.

The rest of the paper is organized as follows. In the following Section the governing equations are introduced. Section 3 reviews the main elements of the dG and of the generalized Cranck-Nicolson method. In Section 4 are shown some first numerical results performed on two bi-dimensional unsteady viscous test-case: the Taylor-Green vortex and the double shear layer. The last Section is devoted to conclusions, remarks and possible future developments.

2 GOVERNING EQUATIONS

The governing equations of compressible viscous flows are the Navier-Stokes equations, written here using Einstein notation:

$$\begin{aligned}
&\frac{\partial \rho}{\partial t} + \frac{\partial}{\partial x_j}\left(\rho u_j\right) = 0, \\
&\frac{\partial}{\partial t}\left(\rho u_i\right) + \frac{\partial}{\partial x_j}\left(\rho u_j u_i\right) = -\frac{\partial p}{\partial x_i} + \frac{\partial \tau_{ji}}{\partial x_j}, \\
&\frac{\partial}{\partial t}\left(\rho E\right) + \frac{\partial}{\partial x_j}\left(\rho u_j H\right) = \frac{\partial}{\partial x_j}\left[u_i \tau_{ij} - q_j\right].
\end{aligned} \tag{1}$$

In these equations, $i, j = 1, \ldots, d$, where $d \in 2, 3$ is the geometrical dimension of the problem, E and H are the total energy and the total enthalpy, respectively, and the pressure, stress tensor and heat flux vector are given by:

$$p = (\gamma - 1)\,\rho\left(E - \frac{u_k u_k}{2}\right), \quad \tau_{ij} = 2\mu\left[S_{ij} - \frac{1}{3}\frac{\partial u_k}{\partial x_k}\delta_{ij}\right], \quad q_j = -\frac{\mu}{Pr}\frac{\partial h}{\partial x_j}, \tag{2}$$

where $\gamma = cp/cv$, Pr is the molecular Prandtl number and S_{ij} is the mean strain-rate tensor, that is:

$$S_{ij} = \frac{1}{2}\left(\frac{\partial u_i}{\partial u_j} + \frac{\partial u_j}{\partial x_i}\right). \tag{3}$$

In order to ensure the entropy conserving/stable property in space, we introduce the set of entropy variables:

$$\mathbf{v} = \left\{\frac{\gamma - s}{\gamma - 1} - \beta|\mathbf{u}|^2,\ \frac{\rho u_1}{p},\ \frac{\rho u_2}{p},\ -\frac{\rho}{p}\right\}, \tag{4}$$

in which, s is the physical entropy, *i.e.* $s = \ln(p\rho^{-\gamma})$ and $\beta = \rho/(2p)$, and we rewrite the system (1) in terms of entropy variables, in a more compact form, as:

$$\mathbf{P}(\mathbf{v})\frac{\partial \mathbf{v}}{\partial t} + \nabla \cdot \mathbf{F}_c(\mathbf{v}) + \nabla \cdot \mathbf{F}_v(\mathbf{v}, \nabla \mathbf{v}) = \mathbf{0}, \tag{5}$$

where $\mathbf{F}_c$ and $\mathbf{F}_v$ are the convective and the viscous flux functions, respectively, and $\mathbf{P}\left(\mathbf{v}\right)$ is the matrix that takes into account of the change of variables from the conservative set, $\mathbf{q} = (\rho, \rho u_i, \rho E)$, to the entropy set $\mathbf{v}$, which is symmetric positive-definite.

3 SPACE AND TIME DISCRETIZATION

Following the method of lines here adopted, we first consider the dG approximation based on the spaces:

$$\mathbb{P}_d^k(\mathcal{K}_h) \stackrel{\text{def}}{=} \left\{v_h \in L^2(\Omega)\,|\,v_{h|K} \in \mathbb{P}_d^k(K),\ \forall K \in \mathcal{K}_h\right\}, \tag{6}$$

where k is a non-negative integer, $d \in 2, 3$ is the geometrical dimension of the problem, $\mathcal{K}_h = \{K\}$ is a mesh of the domain $\Omega \in \mathbb{R}^d$, consisting of non-overlapping elements K such that

$$\Omega_h = \bigcup_{K \in \mathcal{K}_h} K, \tag{7}$$

and $\mathbb{P}_d^k$ denotes the restriction to K of the polynomial functions of d variables and total degree $\leq k$. For this polynomial space, according to [26], is here considered a set of orthonormal and hierarchical basis functions, local to each element, and defined on the physical space.

Denoting with $\mathbf{F}$ the sum of the convective and viscous flux function, and by using the BR2 scheme proposed in [27], to which the interested reader is referred for further information, the dG formulation of Eq.s (5) , is given by

$$\begin{aligned}\sum_{K\in\mathcal{K}_h}\int_K \phi_i P_{j,k}\left(\mathbf{v}_h\right)\phi_l\frac{dV_{k,l}}{dt}d\mathbf{x} - \sum_{K\in\mathcal{K}_h}\int_K \frac{\partial\phi_i}{\partial x_n}F_{j,n}\left(\mathbf{v}_h,\nabla_h\mathbf{v}_h+\mathbf{r}\left(\left[\!\left[\mathbf{v}_h\right]\!\right]\right)\right)d\mathbf{x} \\ + \sum_{F\in\mathcal{F}_h}\int_F \left[\!\left[\phi_i\right]\!\right]_n \widehat{F}_{j,n}\left(\mathbf{v}_h^{\pm},\left(\nabla_h\mathbf{v}_h+\eta_F\mathbf{r}_F\left(\left[\!\left[\mathbf{v}_h\right]\!\right]\right)\right)^{\pm}\right)d\sigma = \mathbf{0},\end{aligned} \tag{8}$$

for $i=1,\ldots,N_{dof}$, where repeated indices imply summation over the ranges $k=1,\ldots,d+2$, $l=1,\ldots,N_{dof}$ and $n=1,\ldots,d$. In the above equations, $\mathbf{r}\left[\!\left[\mathbf{v}_h\right]\!\right]$ and $\mathbf{r}_F\left(\left[\!\left[\mathbf{v}_h\right]\!\right]\right)$ are the global and the local lifting operator, respectively, which arise from the BR2 dG discretization of the viscous fluxes, $\mathbf{v}_h$ is a finite element approximation of the solution $\mathbf{v}$ that belongs to the discrete space $\mathbf{V}_h \stackrel{\text{def}}{=} \left[\mathbb{P}_d^k\left(\mathcal{K}_h\right)\right]^{d+2}$, $\mathcal{F}_h$ is the set of the mesh faces defined as $\mathcal{F}_h \stackrel{\text{def}}{=} \mathcal{F}_h^i \cup \mathcal{F}_h^b$, where $\mathcal{F}_h^i$ collects the internal faces of Ω_h and $\mathcal{F}_h^b$ the faces located on the boundary of Ω_h.

The convective numerical flux is computed from the solution of exact or approximated local Riemann problems in the normal direction at each integration point on elements faces. In the present work, to compute this term, we use the entropy stable exact Riemann solver of Gottlieb and Groth [28], labelled ERS in Section 4, and the entropy conservative flux of Ismail and Roe [11], labelled EC in the same Section.

Moreover, it is important to highlight that, following the approach of Hughes *et al.* [5], the system (8) is here numerically solved directly approximating the entropy variables $\mathbf{v}$ in the dG discrete polynomial space. This means that the integrals must be computed exactly to fulfill the entropy conservation property but, in practice, at the discrete level, integrals are numerically approximated via quadrature rules, *e.g.* Gaussian rules. The numerical results presented in [29] have shown that, by exploiting the over-integration technique, the entropy conservation property can be verified also at the discrete level.

Rewriting the semi-discrete system (8) for a single element K, we obtain the following compact form:

$$\int_K \phi_i \mathbf{P}(\mathbf{v}_h)\frac{d\mathbf{v}_h}{dt}d\mathbf{x} = \mathbf{R}\left(\mathbf{v}_h\right), \tag{9}$$

that is used to advance the solution in time when standard time integration methods are employed, that is, in this work, the standard Crank-Nicolson scheme [30], labelled SCN in Section 4, and the explicit three-stage, third-order accurate Runge-Kutta scheme [31], labelled RK33 in the same Section. In particular, when the standard Crank-Nicolson scheme is used, the following system of algebraic equations is solved:

$$\int_K \phi_i \mathbf{P}\left(\mathbf{v}_h^{n+1/2}\right)\frac{\mathbf{v}_h^{n+1}-\mathbf{v}_h^n}{\Delta t}d\mathbf{x} = \mathbf{R}\left(\mathbf{v}_h^{n+1/2}\right), \tag{10}$$

where $\mathbf{v}_h^{n+1/2} = 1/2(\mathbf{v}_h^{n+1}+\mathbf{v}_h^n)$.

On the contrary, to preserve the entropy conservation/stable property for time dependent problems, the entropy conserving Crank-Nicolson method is used. This time integration method, labelled GCNG in Section 4, is an extension of the generalized Crank-Nicolson method originally proposed in [16, 20] in the contest of a Finite Volume method and conservative working variables. Inspired by the above cited works, we have advanced the solution in time in each K element as follows:

$$\int_K \phi_i \frac{\mathbf{q}_h^{n+1} - \mathbf{q}_h^n}{\Delta t} d\mathbf{x} = \mathbf{R}\left(\mathbf{v}_h^{n+1/2}\right), \tag{11}$$

where $\mathbf{q}_h^n$ is the projection on the dG space of the conservative variables computed from the entropy ones, that is:

$$\int_K \phi_i \mathbf{q}_h^n d\mathbf{x} = \int_K \phi_i \mathbf{q}\left(\mathbf{v}_h^n\right) d\mathbf{x}, \tag{12}$$

and $\mathbf{v}_h^{n+1/2}$ is a temporal intermediate state computed as suggested in [21], that is, for the bi-dimensional problems here investigated:

$$\begin{aligned}
v_1^{n+1/2} &= \frac{1}{\gamma - 1}\left(\gamma \frac{\bar{\rho}}{\rho^{\ln}} - \bar{s}\right) - \bar{u}_1 v_2^{n+1} - \bar{u}_2 v_3^{n+1} - \frac{1}{2}\left|\bar{\mathbf{u}}\right|^2 v_4^{n+1}, \\
v_2^{n+1/2} &= -\bar{u}_1 v_4^{n+1}, \\
v_3^{n+1/2} &= -\bar{u}_2 v_4^{n+1}, \\
v_4^{n+1/2} &= -\frac{\bar{\rho}}{p^{\ln}},
\end{aligned} \tag{13}$$

where the bar symbol denotes the arithmetic average of the variables computed at the time levels n and $n+1$, and the log state of density and pressure is computed as:

$$\circ^{\ln} = \frac{\circ^{n+1} - \circ^n}{\log \circ^{n+1} - \log \circ^n}. \tag{14}$$

For the proof of the entropy conservation property of this time integration method and further details about its implementation, the interested reader can refer to [24].

4 NUMERICAL RESULTS

In this section are presented the first results obtained for two viscous bi-dimensional unsteady nearly incompressible test-case: the Taylor-Green vortex and the double shear layer. Several simulations are performed to evaluate the performance of the GCNG time integration method with respect to the RK33 explicit scheme, and to assess its order of convergence an its accuracy. Furthermore, the robustness of the proposed numerical framework, when the EC or ES fluxes are used, has been investigated.

4.1 The viscous Taylor-Green vortex

The bi-dimensional viscous Taylor-Green vortex [32] has the following exact solution for incompressible flows:

$$\begin{aligned} p &= p_0 + \frac{\rho_0 V_0^2}{4}\left(\cos(2x)+\cos(2y)\right)e^{-4\nu t} \quad , \\ u_1 &= V_0 \sin(x)\cos(y)e^{-2\nu t}, \\ u_2 &= -V_0 \cos(x)\sin(y)e^{-2\nu t}, \\ T &= 1, \end{aligned} \tag{15}$$

where $p_0 = \rho_0 = 1$ and $V_0 = M_\infty\sqrt{\gamma}$. Note that the initial flow field is obtained substituting in the above equations $t = 0$. The compressibility effects have been minimized by considering a Mach number $M_\infty = 0.1$. Furthermore, we have fixed $Re = 100$. The simulations, that are advanced in time up to t, that is the time corresponding to one vortex revolution, have been performed on a computational domain with $-\pi \leq x, y \leq \pi$, which has been equipped with periodic boundary conditions in the two directions and discretized with a $[10 \times 10]$ uniform Cartesian grid.

To remark why we are looking for an entropy conserving time integration method that possess the good stability property of the implicit methods, it has been made a comparison between the larger time step size usable with GCNG and the one that must be used, for stability reasons, with RK33. The result of this study is that the larger usable time step with GCNG is roughly 400 times larger than the one strictly required by the explicit scheme for stability reasons, *i.e.* $\Delta t_{GCNG} = t/10$, $\Delta t_{RK33} \simeq t/4000$. One can argue that this favourable comparison is due to the small Mach number used for this test-case, that the CPU time per time step is clearly not the same for the two methods, and that the results obtained with GCNG will be less accurate than the ones obtained with RK33. Nevertheless, it is undeniable that a ratio of 400 is a quite large value and that, as highlighted in Fig.1, pressure and velocity components, computed with the implicit and the explicit schemes, are roughly the same.

4.2 The viscous double shear layer

The fully-discrete EC and ES methods are here assessed with a non-smooth test problem, the viscous double shear layer [32, 33], which initial flow field is:

$$\begin{aligned} u_1 &= \begin{cases} U_\infty \tanh\left[\left(y-\pi/2\right)/\delta_1\right] & \text{if } y \leq \pi, \\ U_\infty \tanh\left[\left(3\pi/2-y\right)/\delta_1\right] & \text{if } y > \pi, \end{cases} \\ u_2 &= U_\infty \delta_2 \sin(x), \\ p &= 1 \quad \text{and} \quad T = 1, \end{aligned} \tag{16}$$

where $U_\infty = M_\infty\sqrt{\gamma}$, $\delta_1 = \pi/15$ and $\delta_2 = 0.05$. To obtain a nearly incompressible flow, $M_\infty = 0.01$. Finally, $Re = 500$. The computational domain, defined by $0 \leq x, y \leq 2\pi$, has been discretized with a $[8 \times 8]$ uniform Cartesian grid, all the boundaries are periodic and the simulations are advanced in time up to $t = 8$.

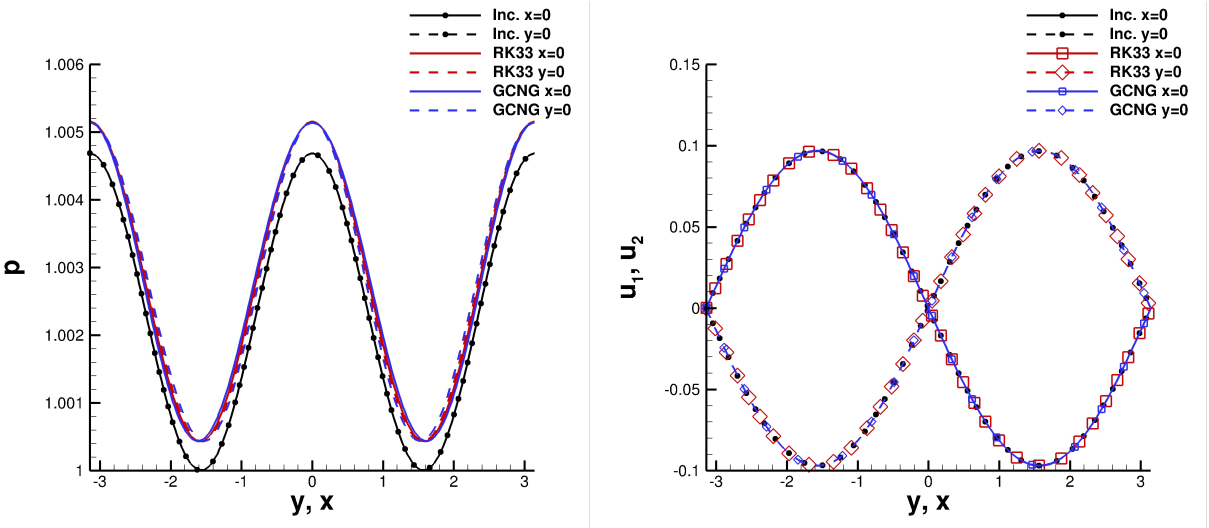

(a) Pressure

(b) Velocity components

Figure 1: Viscous Taylor-Green vortex– Simulations performed with the dG approximation $k = 6$, the ERS flux and GCNG and RK33 time integration methods. Pressure (a) and velocity components (b) along $x = 0$ and $y = 0$ lines. The exact analytical solution of an incompressible flow (black lines) is reported for comparison purpose.

To assess the numerical framework, a time convergence study has been performed, which results are reported in Fig. 2. Since this problem has no analytical solution, the computed convergence rate has been evaluated by using several successively refined solutions, obtained by halving the time step size Δt, and computing the ε variable, which is defined as:

$$\varepsilon = \Omega_h^{-1} \int_{\Omega_h} (\rho \ln \frac{p}{\rho^\gamma}) \, d\Omega. \tag{17}$$

The convergence rate p is then computed as:

$$p = \log_2 \frac{\varepsilon_{\Delta t} - \varepsilon_{\Delta t/2}}{\varepsilon_{\Delta t/2} - \varepsilon_{\Delta t/4}}. \tag{18}$$

Note in fact that, in Fig. 2 on the x-axis of the plot it is reported the arithmetic average of the time step sizes used for two successive simulations, and on the y-axis the absolute value of the difference between the corresponding two ε values obtained, *i.e* $|\varepsilon_{\text{diff}}| = \left|\varepsilon_{\Delta t} - \varepsilon_{\Delta t/2}\right|$. The figure shows that the computed convergence rate of GCNG is equal to the designed order of convergence of 2, independently from the numerical flux used, *i.e.* a conserving (EC) or a stable (ERS) one. Furthermore, in the plot the results obtained with SCN are reported for comparison purpose, highlighting that, as already assessed for inviscid flows [24, 25], the accuracy of the two time integration methods is exactly the same. Quantitative values of the performed time refinement study are reported in Tab. 1, in which only the results obtained with GCNG and ERS flux are reported, since almost identical numerical values are obtained in the other cases.

Another very important aspect that this study has put in evidence, is that the use of the EC flux leads to a divergent solution for the larger time step sizes, independently from the time

integration method used, *i.e.* GCNG or SCN. Note, in fact, that in Fig. 2 the results related to the above cited simulations are not reported.

To better investigate this bad behaviour, a further analysis has been done lowering the number of krylov subspace with respect to the one used to perform the previous simulations. The results of this analysis are reported in Tab.2 for the SCN (left table) and the GCNG (right table) time integration methods. Both the tables show that the use of the EC flux leads to a very poor robustness property of the discretization, which is caused by the failure of the Newton's algorithm when time step sizes typical of implicit methods are used, especially by raising the dG approximation from $k = 1$ up to $k = 6$. Furthermore, by comparing the number of divergent simulations (cross symbol) performed with odd and even dG approximations it is clear that the even dG approximations are less robust than the odd ones, thus confirming the odd/even effect already highlighted in [29] for inviscid flows.

In Tab.3 are shown the results performed with the ES flux, the SCN (left table) and the GCNG (right table) time integration methods. Both the tables clearly show that the simulations are more robust if an entropy stable flux is used. In this case, in fact, it is possible to perform convergent simulations with very large time step size, *e.g.* $\Delta t = t/4$, even ranging the polynomial dG approximation up to $k = 6$.

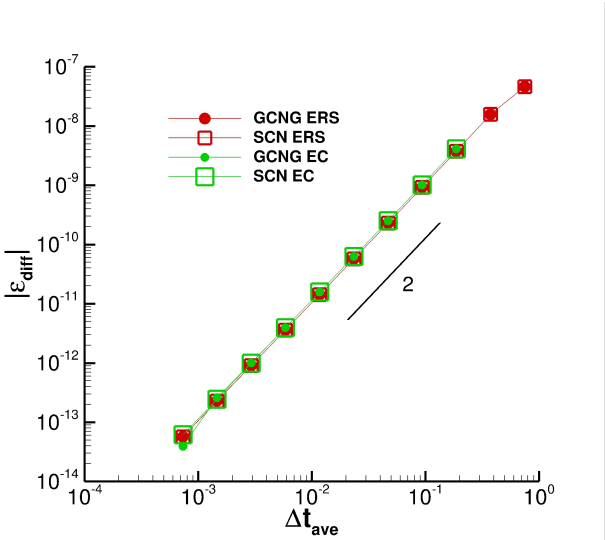

Figure 2: Viscous double shear layer–Simulations performed with the dG approximation $k = 6$, ERS and EC numerical fluxes and GCNG and SCN time integration methods.

5 CONCLUSIONS

In this work are shown the first results obtained for unsteady compressible viscous flows with a fully-discrete entropy conserving/stable discretization. The method here used is the method of lines, based on a high-order modal discontinuous Galerkin (dG) method in space and an implicit second order accurate discretization in time. In particular, in order to obtain an entropy conserving/stable scheme in space, the dG approximation has been equipped with entropy working variables and entropy conservative and stable numerical fluxes. Furthermore, in order to ob-

Δt	Δt_{ave}	ε	$\varepsilon_{\text{diff.}}$	p
$t/8$	$7.5 \cdot 10^{-1}$	$1.4039532257 \cdot 10^{-6}$	$-4.5935121284 \cdot 10^{-8}$	
$t/16$	$3.75 \cdot 10^{-1}$	$1.4498883470 \cdot 10^{-6}$	$-1.5792012211 \cdot 10^{-8}$	1.54
$t/32$	$1.875 \cdot 10^{-1}$	$1.4656803592 \cdot 10^{-6}$	$-3.7436001683 \cdot 10^{-9}$	2.08
$t/64$	$9.375 \cdot 10^{-2}$	$1.4694239593 \cdot 10^{-6}$	$-9.2119417146 \cdot 10^{-10}$	2.02
$t/128$	$4.6875 \cdot 10^{-2}$	$1.4703451535 \cdot 10^{-6}$	$-2.2901225419 \cdot 10^{-10}$	2.01
$t/256$	$2.34375 \cdot 10^{-2}$	$1.4705741658 \cdot 10^{-6}$	$-5.7194729370 \cdot 10^{-11}$	2.00
$t/512$	$1.171875 \cdot 10^{-2}$	$1.4706313605 \cdot 10^{-6}$	$-1.4339451880 \cdot 10^{-11}$	2.00
$t/1024$	$5.859375 \cdot 10^{-3}$	$1.4706456700 \cdot 10^{-6}$	$-3.6022494600 \cdot 10^{-12}$	1.99
$t/2048$	$2.9296875 \cdot 10^{-3}$	$1.4706493022 \cdot 10^{-6}$	$-9.0056939999 \cdot 10^{-13}$	2.00
$t/4096$	$1.46484375 \cdot 10^{-3}$	$1.4706502028 \cdot 10^{-6}$	$-2.3025557990 \cdot 10^{-13}$	1.97
$t/8192$	$7.32421875 \cdot 10^{-4}$	$1.4706504330 \cdot 10^{-6}$	$-5.6911049995 \cdot 10^{-14}$	2.02
$t/16384$		$1.4706504899 \cdot 10^{-6}$		

Table 1: Viscous double shear layer–Simulations performed with the dG approximation $k = 6$, ERS flux and GCNG time integration method.

tain a fully-discrete entropy conserving/stable scheme, the generalized Crank-Nicolson method, originally proposed in [20, 16], has been here extended to the dG approximation with entropy variables. The numerical results, obtained for two bi-dimensional unsteady viscous test case, have confirmed the convergence rate of 2 of the time integration method and the odd/even effect of the dG approximation when an entropy conserving flux is used, already highlighted in [29] for inviscid flows. Furthermore, when an entropy conserving flux is used, the numerical results show a very difficult convergence of the Newton's algorithm. Nevertheless, it is important to notice that, despite the general fast convergence of Newton's method, it has various drawbacks that can cause its failure or a slow convergence, *e.g*: initial guess too far from the searched solution, near local maxima and local minima, multiple roots etc. Future work will be devoted to include more advanced Newton-like solvers based on the nonlinear solvers SNES included in the PETSc library [34].

REFERENCES

[1] E. Tadmor, Numerical viscosity and the entropy condition for conservative difference schemes, Mathematics of Computation 43 (1984) 369–381.

[2] E. Tadmor, A minimum entropy principle in the gas dynamics equations, Applied Numerical Mathematics 2 (1986) 211–219.

[3] E. Tadmor, The numerical viscosity of entropy stable schemes for systems of conservation laws. I, Mathematics of Computation 49 (1987) 91–103.

[4] A. Harten, On the symmetric form of systems of conservation laws with entropy, Journal of Computational Physics 49 (1983) 151–164.

[5] T. Hughes, L. Franca, M. Mallet, A new finite element formulation for computational fluid dynamics: I. symmetric forms of the compressible euler and navier-stokes equations and the

SCN

Δt \ k	1	2	3	4	5	6
$t/2$	×	×	×	×	×	×
$t/4$	×	×	×	×	×	×
$t/8$	•	×	•	×	×	×
$t/16$	•	•	•	×	•	×
$t/32$	•	•	•	×	•	×
$t/64$	•	•	•	×	•	×
$t/128$	•	•	•	×	•	×
$t/256$	•	•	•	•	•	×
$t/512$	•	•	•	•	•	•

GCNG

Δt \ k	1	2	3	4	5	6
$t/2$	×	×	×	×	×	×
$t/4$	•	×	×	×	×	×
$t/8$	•	×	•	×	×	×
$t/16$	•	•	•	×	•	×
$t/32$	•	•	•	×	•	×
$t/64$	•	•	•	×	•	×
$t/128$	•	•	•	×	•	×
$t/256$	•	•	•	•	•	×
$t/512$	•	•	•	•	•	•

Table 2: Viscous double shear layer–Simulations performed with EC flux, dG approximations ranging from $k = 1$ up to $k = 6$ and the time integration methods SCN (left table) and GCNG (right table). The cross ans bullet symbols denote a divergent and a convergent simulation, respectively.

SCN

Δt \ k	1	2	3	4	5	6
$t/2$	•	•	×	×	×	×
$t/4$	•	•	•	•	•	•

GCNG

Δt \ k	1	2	3	4	5	6
$t/2$	•	•	×	×	×	×
$t/4$	•	•	•	•	•	•

Table 3: Viscous double shear layer–Simulations performed with ES flux, dG approximations ranging from $k = 1$ up to $k = 6$ and the time integration methods SCN (left table) and GCNG (right table). The cross ans bullet symbols denote a divergent and a convergent simulation, respectively.

second law of thermodynamics, Computer Methods in Applied Mechanics and Engineering 54 (1986) 223–234.

[6] J. Manzanero, G. Rubio, E. Ferrer, E. Valero, Dispersion-dissipation analysis for advection problems with nonconstant coefficients: Applications to discontinuous galerkin formulations., SIAM Journal of Scientific Computing 40 (2018) A747—-A76.

[7] G. Gassner, D. Kopriva, A comparison of the dispersion and dissipation errors of gauss and gauss–lobatto discontinuous galerkin spectral element methods, SIAM Journal of Scientific Computing 33 (2011) 2560–2579.

[8] G. Jang, C.-W. Shu, On a cell entropy inequality for discontinuous galerkin methods, Mathematics of computation 62 (1994) 531–538.

[9] G. Gassner, A. Winters, A novel robust strategy for discontinuous galerkin methods in computational fluid mechanics: Why? when? what? where?, Frontiers in Physics 8:500690. doi:10.3389/fphy.2020.500690.

[10] P. Chandrashekar, Kinetic energy preserving and entropy stable finite volume schemes for compressible Euler and Navier-Stokes equations, Communications in Computational Physics 14 (5) (2013) 1252–1286.

[11] F. Ismail, P. Roe, Affordable, entropy-consistent Euler flux functions II: Entropy production at shocks, Journal of Computational Physics 228 (15) (2009) 5410–5436.

[12] H. Ranocha, Comparison of some entropy conservative numerical fluxes for the euler equations, Journal of Scientific Computing 76 (1) (2018) 216–242.

[13] T. J. Barth, Numerical Methods for Gasdynamic Systems on Unstructured Meshes, Springer Berlin Heidelberg, Berlin, Heidelberg, 1999, pp. 195–285.

[14] A. Hiltebrand, S. Mishra, Entropy stable shock capturing space–time discontinuous Galerkin schemes for systems of conservation laws, Numerische Mathematik 126 (1) (2014) 103–151.

[15] L. T. Diosady, S. M. Murman, Tensor-product preconditioners for higher-order space–time discontinuous Galerkin methods, Journal of Computational Physics 330 (2017) 296–318.

[16] P. G. LeFloch, J. M. Mercier, C. Rohde, Fully discrete, entropy conservative schemes of arbitrary order, SIAM Journal on Numerical Analysis 40 (5) (2003) 1968–1992.

[17] T. C. Fisher, M. H. Carpenter, High-order entropy stable finite difference schemes for nonlinear conservation laws: Finite domains, Journal of Computational Physics 252 (2013) 518–557.

[18] G. J. Gassner, A. R. Winters, D. A. Kopriva, Split form nodal discontinuous Galerkin schemes with summation-by-parts property for the compressible Euler equations, Journal of Computational Physics 327 (2016) 39 – 66.

[19] G. Gassner, A. Winters, F. H. et al., The br1 scheme is stable for the compressible navier–stokes equations, Journal of Scientific Computing 77 (2018) 154–200.

[20] E. Tadmor, Entropy stability theory for difference approximations of nonlinear conservation laws and related time-dependent problems, Acta Numerica 12 (2003) 451–512.

[21] A. Gouasmi, S. M. Murman, K. Duraisamy, Entropy conservative schemes and the receding flow problem, Journal of Scientific Computing 78 (2) (2019) 971–994. doi:10.1007/s10915-018-0793-8.

[22] H. Zakerzadeh, U. S. Fjordholm, High-order accurate, fully discrete entropy stable schemes for scalar conservation laws, IMA Journal of Numerical Analysis 36 (2) (2015) 633–654.

[23] H. Ranocha, L. Dalcin, M. Parsani, Fully discrete explicit locally entropy-stable schemes for the compressible euler and navier–stokes equations, Computers & Mathematics with Applications 80 (5) (2020) 1343–1359.

[24] A. Colombo, A. Crivellini, A. Nigro, Entropy conserving implicit time integration in a Discontinuous Galerkin solver in entropy variables, Submitted to Journal of Computational Physics.

[25] A. Nigro, A. Crivellini, A. Colombo, Fully discrete entropy conserving/stable discontinuous galerkin discretization of the euler equations in entropy variables, To appear in the proceedings of International Conference on Spectral and High Order Methods. ICOSAHOM2021, 12-16th July 2021-Vienna, Austria.

[26] F. Bassi, L. Botti, A. Colombo, D. A. Di Pietro, P. Tesini, On the flexibility of agglomeration based physical space discontinuous Galerkin discretizations, Journal of Computational Physics 231 (1) (2012) 45–65.

[27] F. Bassi, S. Rebay, G. Mariotti, S. Pedinotti, M. Savini, A high-order accurate discontinuous finite element method for inviscid and viscous turbomachinery flows, in: R. Decuypere, G. Dibelius (Eds.), Proceedings of the 2nd European Conference on Turbomachinery Fluid Dynamics and Thermodynamics, Technologisch Instituut, Antwerpen, Belgium, 1997, pp. 99–108.

[28] J. Gottlieb, C. Groth, Assessment of Riemann solvers for unsteady one-dimensional inviscid flows of perfect gases, Journal of Computational Physics 78 (2) (1988) 437–458.

[29] A. Colombo, A. Crivellini, A. Nigro, On the entropy conserving/stable implicit DG discretization of the Euler equations in entropy variables, Computers & Fluids 232 (2022) 105198. doi:https://doi.org/10.1016/j.compfluid.2021.105198.

[30] J. Crank, P. Nicolson, A practical method for numerical evaluation of solutions of partial differential equations of the heat conduction type, Mathematical Proceedings of the Cambridge Philosophical Society 43 (1) (1947) 50–67.

[31] R. J. Spiteri, S. J. Ruuth, A new class of optimal high-order strong-stability-preserving time discretization methods, SIAM Journal on Numerical Analysis 40 (2) (2002) 469–491.

[32] M. Tavelli, M. Dumbser, A staggered space–time discontinuous Galerkin method for the incompressible Navier–Stokes equations on two-dimensional triangular meshes, Computers & Fluids 119 (2015) 235–249.

[33] J. B. Bell, P. Colella, H. M. Glaz, A second-order projection method for the incompressible Navier-Stokes equations, Journal of Computational Physics 85 (2) (1989) 257–283.

[34] S. Balay, S. Abhyankar, M. F. Adams, J. Brown, P. Brune, K. Buschelman, L. Dalcin, A. Dener, V. Eijkhout, W. D. Gropp, D. Kaushik, M. G. Knepley, D. A. May, L. C. McInnes, R. T. Mills, T. Munson, K. Rupp, P. Sanan, B. F. Smith, S. Zampini, H. Zhang, H. Zhang, PETSc Web page (2018).
URL `http://www.mcs.anl.gov/petsc`